Orbit of the Patroclus–Menoetius Binary System and Predictions for the 2024/2025 Mutual Events Season

Marina Brozović, Robert A. Jacobson, Ryan S. Park, Pascal Descamps, Jérôme Berthier, Noemí Pinilla-Alonso, Marcel Popescu, Javier Licandro

The Astronomical Journal, 167:104 (12pp), 2024 March https://doi.org/10.3847/1538-3881/ad1f6e

Orbit of the Patroclus–Menoetius Binary System and Predictions for the 2024/2025 Mutual Events Season

Marina Brozović[1], Robert A. Jacobson[1], Ryan S. Park[1], Pascal Descamps[2], Jérôme Berthier[2], Noemí Pinilla-Alonso[3], Marcel Popescu[4], and Javier Licandro[5,6]
[1] Jet Propulsion Laboratory, California Institute of Technology, 4800 Oak Grove Drive, MC 301-120, Pasadena, CA 91109-8099, USA
marina.brozovic@jpl.nasa.gov
[2] Institut de Mécanique Céleste et de Calcul des Éphémérides, Observatoire de Paris, UMR8028 CNRS, 77 av. Denfert-Rochereau, 75014 Paris, France
[3] Florida Space InstituteUniversity of Central Florida 12354 Research Parkway, Orlando, FL 32826-0650, USA
[4] Astronomical Institute of the Romanian Academy, 5 Cuitul de Argint, 040557 Bucharest, Romania
[5] Instituto de Astrofísica de Canarias (IAC), C/Vía Láctea s/n, E-38205 La Laguna, Tenerife, Spain
[6] Departamento de Astrofísica, Universidad de La Laguna, E-38206 La Laguna, Tenerife, Spain
Received 2023 June 23; revised 2024 January 3; accepted 2024 January 15; published 2024 February 13

Abstract

We report on the ephemeris development for Menoetius, the satellite of Patroclus. Our data set consisted of ground–based and Hubble Space Telescope relative astrometry, as well as 42 lightcurves from the mutual events seasons in 2007, 2012, and 2017/2018. Our dynamical model included the effects of oblate, nonspherical shapes of the components, and we assumed that Menoetius contained ∼22% of the system's mass. We numerically integrated the equations of motion and obtained a set of dynamical parameters that fit the data. We report the fit results in terms of residuals, state vectors, orbital elements and their 1σ uncertainties. The mean osculating semimajor axis is $a = 692.5 \pm 4.0$ km, the mean eccentricity is $e = 0.004 \pm 0.004$, and the International Celestial Reference Frame pole direction in R.A. and decl. is R. A. $= 178.0 \pm 0.5$ deg, $\delta = -74.1 \pm 0.2$ deg. We determined the siderial orbital period of $P = 4.282753 \pm 0.000023$ days. The fit yielded the system $GM = 0.0950 \pm 0.0012$ km^3 s^{-2}, which, in combination with the system volume determined from the stellar occultation and the assumed volume uncertainty of 20%, suggests a system bulk density of 1.05 ± 0.21 g cm^{-3}(1σ). The next season of mutual events starts in February of 2024 and lasts until January of 2025. The Patroclus system is in opposition for the observers on Earth in late September and is suitable for observations of the mutual events with an edge-on geometry in October.

Unified Astronomy Thesaurus concepts: Jupiter trojans (874); Orbital elements (1177); Asteroid satellites (2207)

Supporting material: machine-readable tables

1. Introduction

Patroclus and Menoetius are components of the Trojan binary system located in Jupiter's L5 swarm. The system revolves around the Sun with an 11.9 yr period in an eccentric ($e = 0.14$) and inclined ($i = 22$ deg with respect to the ecliptic) orbit. NASA's LUCY mission is scheduled to fly by the binary in 2033 March. Patroclus was the first binary discovered in Trojan population (Merline et al. 2001). Shortly after its discovery, Merline et al. (2002) reported on a preliminary orbit fit for the satellite with a semimajor axis $a = 610$ km, an orbital period $P = 3.41$ days, and a system mass of $M_{\rm sys} = 87 \times 10^{16}$ kg. They also gave the first estimate of the bulk density of the system, $\rho = 1.3 \pm 0.5$ g cm^{-3}. The low density implied a composition dominated by water ice, or alternatively, a silicate-rich composition with moderate porosity. The low density also suggested that the system's origin is likely the trans-Neptunian region (Morbidelli et al. 2005). Noll et al. (2008) and Nesvorný et al. (2010) proposed that outer solar system binaries formed from collapsing clouds of granular material or through capture events. The nearly equal mass of the two components suggests that the first scenario is more likely. Furthermore, the two components appear to have equal composition and surface properties (Mueller et al. 2010).

Marchis et al. (2006) published a refined orbit based on the data arc from 2001 to 2005. The Keplerian solution was used over the entire length of the data arc, and there were no indications that the orbit was precessing. They reported a roughly circular orbit with an eccentricity of $e = 0.02 \pm 0.02$, a semimajor axis of $a = 680 \pm 20$ km, and an orbital period of $P = 4.283 \pm 0.004$ days. The near-zero eccentricity suggested that this is a tidally evolved system; a tidally evolved satellite can remain in a synchronous, eccentric orbit as long as its shape evokes a permanent quadrupole moment (Murray & Dermott 1998; their Equation (5.95)). Marchis et al. (2006) constrained the location of the orbit pole at the J2000 ecliptic longitude and latitude of $\lambda = 234 \pm 5$ deg and $\beta = -62 \pm 1$ deg ($RA = 179.4$ deg, $\delta = -74.0$ deg). The system mass, $M_{\rm sys} = 1.36 \pm 0.11 \times 10^{18}$ kg, and the preliminary size estimates for the components, $R_P = 60.9 \pm 1.6$ km and $R_M = 56.3 \pm 1.6$ km, yielded a bulk density of $\rho = 0.8^{+0.2}_{-0.1}$ g cm^{-3}.

Mueller et al. (2010) obtained mid-infrared observations of the system undergoing mutual events with the Spitzer Space Telescope. The subsequent thermal modeling resulted in diameters of 106 ± 11 km and 98 ± 10 km for Patroclus and Menoetius respectively. This study also found that the rotation periods for each component were equal to the period of the mutual orbit, thus confirming that the system is fully synchronized.

Buie et al. (2015) reported on the first stellar occultation in October of 2013. This event allowed the direct measurement of the sizes of both components. Patroclus and Menoetius were estimated to be ellipsoids with plane-of-sky dimensions of

124.6 × 92.8 km and 117.2 × 93.0 km. Buie et al. (2015) also obtained three-dimensional shape models for both components based on the lightcurves and occultation cords. The mean-ellipsoidal axes for Patroclus were 127 × 117 × 98 km, and for Menoetius, 117 × 108 × 90 km. The oblate shapes of the components suggest a faster rotation rate in the early history of the system. The binary components likely formed much closer together and then tidally evolved to a separation of approximately 12 primary radii.

The Patroclus–Menoetius mutual event seasons occur about twice per the system's 12 yr orbital period around the Sun. Berthier et al. (2020) reported on 16 lightcurves from the 2007 and 2012 season, and Pinilla-Alonso et al. (2022) reported on five mutual events from the 2017 to 2018 season. Such lightcurves impose powerful constrains on orbital parameters, as well as on the shapes and relative sizes of the components. Berthier et al. (2020) went through an iterative procedure of estimating mean motion, separations, the system pole, and the shapes and relative sizes of the components. The fundamental assumption was a fully synchronous system with a circular orbit, and the components were modeled as heterogeneous Roche equilibrium ellipsoids. The astrometric observations from Grundy et al. (2018) were used to obtain the physical scale for separations between Patroclus and Menoetius. This also yielded absolute dimensions for the shapes of ellipsoids, 130.8 ×126.2 × 122.8 km and 117.1 × 110.8 × 107.8 km. The bulk density was estimated to be $0.81 \pm 0.16\ \mathrm{g\ cm^{-3}}$. The lower density was likely a consequence of ∼24% larger volume than estimated by Buie et al. (2015). This analysis refined the siderial period of the system to $P = 4.282760 \pm 0.000005$ days and determined the orbit pole at R. A. $= 179.1 \pm 0.9$ deg and $\delta = -74.7 \pm 0.1$ deg. For comparison, Grundy et al. (2018) performed an orbit fit based on the 2013–2017 Keck and HST relative astrometry, obtaining $P = 4.282680 \pm 0.000063$ days, $a = 688.5 \pm 4.7$ km, and the orbit pole at R. A. $= 179.3 \pm 1.8$ deg and $\delta = -74.11 \pm 0.60$ deg.

Pinilla-Alonso et al. (2022) reported on five mutual events from the 2017 to 2018 season. The orbit fit by Grundy et al. (2018) was used as a starting point for an orbital update to the newly obtained lightcurves, but this fit did not contain any other data. The shape of a particular lightcurve, where Menoetius was eclipsing Patroculus, suggests that there is a large crater on the south pole of Menoetius. This is consistent with Buie et al. (2015) finding that there were two cords on the body of Menoetius where the stellar occultation was expected, but not detected.

Here we present an orbit fit that was motivated by a long astrometric data arc from 2001 to 2017 and the abundant set of lightcurves. All recent orbital fits, Grundy et al. (2018), Berthier et al. (2020), and Pinilla-Alonso et al. (2022) used subsets of the available data. Our software is capable of modeling both relative astrometry and lightcurves, and simultaneously finding an orbit solution that fits them all. Our dynamical model includes shape-derived gravity coefficients J_2 and C_{22} for both components.

Following the fit, we were interested in evaluating the conditions for the next mutual events season in 2024–2025. We produced predicts that could help observers organize their campaigns. Finally, we also discuss orbital uncertainties for the system during the LUCY spacecraft flyby.

Table 1
State Vectors with Respect to the System Barycenter

Object	Position (km)	Velocity (km s^{-1})
Patroclus	146.7853178306719	−0.0001229182629089184
	−7.151736403593309	−0.002571124573574138
	−41.88579614433345	0.00000889405707149561 2
Menoetius	−519.7214712200603	0.0004352156018255958
	25.32208956853108	0.009103557943100884
	148.3046664140391	−0.00003149110888355475

Note. The epoch is 2005 February 26 TDB. State vectors have high numerical precision in order to facilitate future orbital integrations.

2. Methods

2.1. Observations

The data set consists of relative measurements of Menoetius with respect to Patroclus in the plane of sky (X, Y), and we also have lightcurves resulting from the system undergoing occultations and eclipses. We found 21 astrometry points from 2001 to 2017, obtained either with the Maunakea Keck telescope or with the Hubble Space Telescope (Merline et al. 2001; Marchis et al. 2006; Grundy et al. 2018). The 2013 data point was based on a stellar occultation described in Buie et al. (2015), and it was reported as relative separation in the plane of sky in Grundy et al. (2018). The data obtained in 2013 and 2017 have 2–3 mas precision. At Patroclus' average distance from Earth, 1 mas corresponds to ∼3.9 km. This means that the latest astrometry can pinpoint the location of Menoetius to within 10 km with respect to Patroclus. The older data have the uncertainties in the realm of a few tens of mas, or equivalent to several tens of km.

We include 42 lightcurves from the mutual events observed in 2007, 2012, and 2017/2018. We used 16 lightcurves published in Berthier et al. (2020), as well as 19 additional lightcurves from the same observing campaign. We found that these additional lightcurves still contained either partial or complete lightcurves of the mutual events, and that they can be useful for orbit determination. We also used seven lightcurves (five different events) published from the latest 2017–2018 mutual events season (Pinilla-Alonso et al. 2022). We used observer reported photometric errors when available, and we scaled each lightcurve contribution to the χ^2 of the fit with respect to the number of points.

We modeled the shapes of lightcurves with the Dunbar & Tedesco (1986) three-circle overlap model. The model uses three circles to represent Patroclus, Menoetius, and the shadow of either Patroclus or Menoetius. The model is simple but effective, and we found it sufficient for orbit fitting. Brozović et al. (2015) also employed this approach for the orbit fit of Charon in order to model lightcurves from the Pluto–Charon mutual events.

Mutual events occur in the plane perpendicular to the observer's line of sight to the eclipsed/occulted body. The model calculates the surface area, ΔA, that is affected by the disk of the occulting body and/or the shadow belonging to that body. We performed separate fits of the Patroclus–Menoetius lightcurves using two sets of radii: 49 and 45 km as reported in Grundy et al. (2018), and 56.5 and 52 km, as reported in Buie et al. (2015). The smaller radii correspond to the polar radii from (Buie et al. 2015). It is unlikely that the objects are

Table 2
Residual Statistics

Observation	Site	X_{obs} (arcsecond)	Y_{obs} (arcsecond)	X_{calc} (arcsecond)	Y_{calc} (arcsecond)	$(O-C)_X$ (arcsecond)	$(O-C)_Y$ (arcsecond)	σ_X	σ_Y
2001 09 22 14:43:34	Keck	−0.19800	−0.00680	−0.2260	−0.0747	0.0281	0.0057	0.94	0.57
2001 10 13 11:25:48	Keck	−0.07550	−0.09230	−0.0897	−0.1115	0.0152	0.0183	0.51	0.91
2002 02 06 06:13:09	Keck	−0.09900	−0.11000	−0.0849	−0.0949	−0.0134	−0.0154	−0.67	−0.77
2002 02 07 06:54:11	Keck	−0.15980	−0.01	−0.1790	0.0098	0.0174	−0.0213	0.87	−0.71
2004 11 02 15:23:55	Keck	0.0203	−0.0539	0.0158	−0.0567	0.0054	0.0032	0.27	0.32
2004 11 02 15:29:51	Keck	0.01940	−0.0519	0.0149	−0.0569	0.0054	0.0054	0.27	0.54
2005 02 26 09:46:06	Keck	−0.00750	−0.08250	−0.0028	−0.0902	−0.0040	0.0082	−0.13	0.82
2005 03 01 10:22:53	Keck	0.18600	0.05000	0.1834	0.0478	0.0020	0.0033	0.10	0.17
2005 03 01 10:31:42	Keck	0.1855	0.0425	0.1838	0.0470	0.0011	−0.0035	0.05	−0.17
2005 04 30 06:45:45	Keck	0.1419	0.0523	0.1458	0.0554	−0.0047	−0.0024	−0.23	−0.12
2005 04 30 06:56:21	Keck	0.05230	0.05230	0.1466	0.0548	−0.0005	0.0012	−0.02	0.06
2005 05 28 06:32:54	Keck	−0.1459	−0.0313	−0.1495	−0.0348	0.0037	0.0026	0.18	0.13
2005 05 28 06:38:21	Keck	−0.1469	−0.0311	−0.1497	−0.0345	0.0029	0.0034	0.14	0.11
2005 05 28 06:44:15	Keck	−0.14820	−0.03110	−0.1499	−0.0342	0.0018	0.0032	0.09	0.11
2013 10 21 06:43:00	Keck	−0.2463	−0.0185	−0.2450	−0.0160	−0.0013	−0.0025	−0.42	−0.84
2017 05 20 13:09:00	HST	0.1434	−0.0062	0.1437	−0.0061	−0.0009	−0.0002	−0.46	−0.10
2017 05 29 22:44:00	HST	−0.0194	−0.0585	−0.0146	−0.0590	−0.0057	0.0004	−1.90	0.14
2017 06 08 00:27:00	HST	−0.1138	−0.0498	−0.1142	−0.0498	−0.0002	0.0000	−0.10	−0.01
2017 06 13 12:21:00	HST	−0.0646	0.0356	−0.0700	0.0368	0.0051	−0.0012	1.71	−0.40
2017 06 14 07:25:00	HST	0.0932	0.0542	0.0940	0.0518	−0.0012	0.0025	−0.60	1.23
2017 12 09 14:36:00	Keck	−0.1443	0.0102	−0.1451	0.0091	0.0008	0.0010	0.38	0.52

Note. Residuals for relative astrometry X and Y. The relative measurements represent $X = (\alpha_2 - \alpha_1)\cos(\delta_1)$ and $Y = \delta_2 - \delta_1$ where α is R.A., δ is decl., 1 refers to Patroclus and 2 refers to Menoetius. $(O-C)_X$ and $(O-C)_Y$ represent the absolute difference between the observed (O) and computed (C) data points in arcseconds and σ_X and σ_Y represent the weighted residuals in units of standard deviation. The rms of the absolute residuals are (9 mas, 8 mas) with means of 3 mas and 1 mas. The rms of the weighted residuals are (0.69, 0.54) with the means of 0.05 and 0.12. The measurements were originally reported in Merline et al. (2001), Marchis et al. (2006), and Grundy et al. (2018).

significantly smaller or larger than these two sets. Consequently, these cases represent the upper and lower limits that we later utilized to asses the orbital uncertainties.

The fractional change in the intensity of light was calculated as:

$$F = \frac{\kappa_2 \Delta A}{I_0} = \frac{\kappa_2}{\kappa_1} \frac{\Delta A}{\pi (R_1^2 + \frac{\kappa_2}{\kappa_1} R_2^2) \cos^2(\phi/2)} \quad (1)$$

where ΔA denotes the three-circle overlap area, I_0 is the total uneclipsed intensity (see Dunbar & Tedesco 1986), κ_1 and κ_2 are the albedos of the occulting and the occulted bodies, and R_1 and R_2 are the radii of the occulting and the occulted bodies. The albedo of the occulting body κ_1 was kept equal to one while the albedo of the occulted body κ_2 was treated as a floating parameter and adjusted for the each individual lightcurve. Note that the model fit only depends on the albedo ratio. This model assumes a Lambertian surface, neglecting the center-to-limb brightness distribution. While the model may not be photometrically complete, it is suitable for modeling lightcurves for orbit determination purposes. Arlot et al. (2013) noted that albedo, as opposed to scattering law, is considerably more important when extracting astrometry from a lightcurve. We account for the effect of gibbousness by multiplying I_0 with $\cos^2(\phi/2)$, where ϕ is the phase angle. We note that the largest phase of ∼12 deg occurred for a single (almost flat) lightcurve on 2012 November 28. All other lightcurves had phase angles of less than 10°.

The intensity variation can be expressed in terms of magnitude as:

$$m = V_0 + 2.5 \log_{10}(1 - F). \quad (2)$$

Here, V_0 represents the base magnitude. Additionally, we introduced a linear term in time to account for slopes observed in some of the lightcurves.

2.2. Orbital Model

Previous orbit fits always treated the Menoetius orbit as purely Keplerian, mostly with zero eccentricity. We used a conic model to fit several months of astrometry in order to produce the starting state vector, but we quickly adopted a more complete model of the system. We decided to split the system's mass between the components according to the ratio determined by their volumes (Buie et al. 2015). Assuming the same density for the components, Menoetius contains ∼22% of the system's mass. We also included theoretical values for the gravity coefficients J_2 and C_{22} based on the shapes of the components reported in Buie et al. (2015). We obtained $J_2 = 0.067$ and $C_{22} = 0.0074$ for Menoetius with an equivalent radius of 52 km. Similarly, Patroclus has $J_2 = 0.066$ and $C_{22} = 0.0076$ for an equivalent radius of 56.5 km. Our model also included perturbations from the Sun and Jupiter.

The equations of motion were formulated in the Cartesian coordinate system with the barycenter of the Patroclus–Menoetius system at the origin (Peters 1981). We assumed that the spin vectors of the two bodies were perpendicular to the mutual orbit plane. For numerical integration, we employed

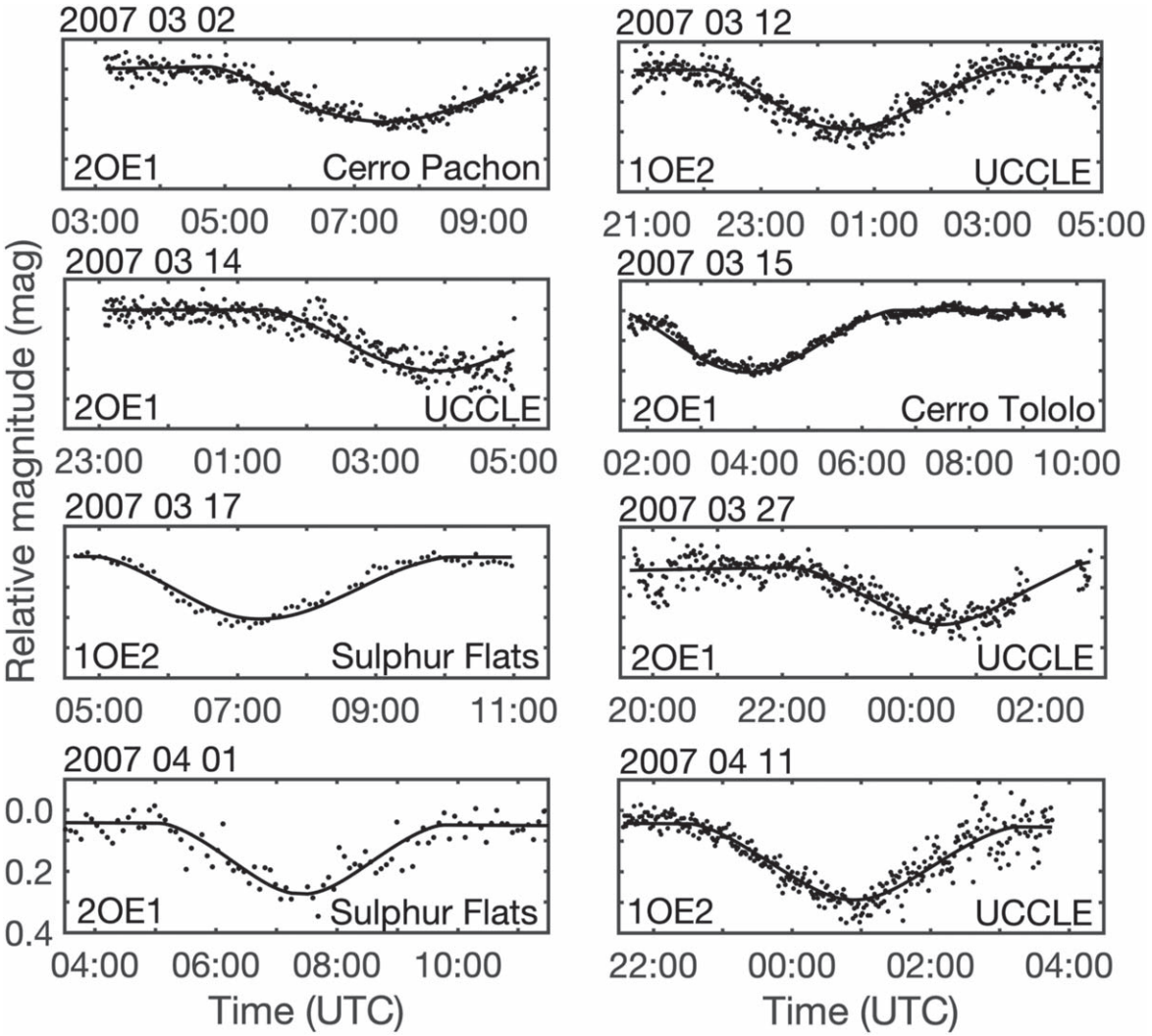

Figure 1. Solid lines represent model fits to the selected mutual events lightcurves from 2007. We adopted the same nomenclature as in Berthier et al. (2020). Index 1 refers to Patroclus and index 2 to Menoetius. We mark the type of an event as O for an occultation and E for an eclipse. The vertical dimension is the same for all panels, 0.5 mag. The rest of the lightcurves fits from 2007 are in the Appendix.

the variable order, variable time step Gauss–Jackson method (Jackson 1924). The average step size used in the integration was 1200 seconds, and the maximum velocity error remained well below the imposed limit of 10^{-10} km s^{-1}. We adopted the International Celestial Reference Frame (ICRF) as the coordinate frame, consistent with the reported astrometry. To maintain consistency with the JPL ephemerides convention, we used Barycentric Dynamical Time (TDB), also known as Temps Dynamique Barycentrique. We used solution number 82 from JPL's On-Line Solar System Data Service to model the heliocentric orbit of the Patroclus system barycenter (Giorgini et al. 1996). The position of the Sun with respect to the solar system barycenter was obtained from the latest DE440 planetary ephemerides (Park et al. 2021). The mass of the Sun was augmented with the masses of Mercury, Venus, Earth–Moon system, and Mars ($GM = 132713233263.4$ km^3 s^{-2}, where GM is mass multiplied by the Newtonian gravitational constant, G).

We went through an iterative procedure in which we first propagated the state vector via the equations of motion to the observed time. The state vectors were used to calculate the observables. We formed separate square root information arrays for the lightcurves and relative astrometry and packed them into a composite array from where we obtained a solution via singular value decomposition (Bierman 1977). The estimation process used a least squares procedure based on Householder transformations (Lawson & Hanson 1974; Tapley et al. 2004) in order to adjust the epoch state vector for the satellite and the system mass.

Taking into account the similarity in size of the two components, the sparse relative astrometry data, and the 4 day orbital period, we took special care to avoid any skipped orbital revolutions. First, we fitted the most abundant set of relative astrometry from 2005, consisting of eight points reported between February 26 and May 28. The orbit epoch was set to 2005 February 26. This ∼90 days data arc yielded the initial mean motion estimate. Next, we extended the data arc by including two points from 2004 November 2 (∼4 months prior). We estimated that mean motion error would have to be at least ∼3.4 deg day^{-1} to skip one full rotation. Lightcurves from March of 2007 were added next. They all had relatively small amplitudes, ranging from 0.2 to 0.3 mag, because the orbital geometry was not completely edge-on. Taken at face value, the similar sizes of Patroclus and Menoetius make it

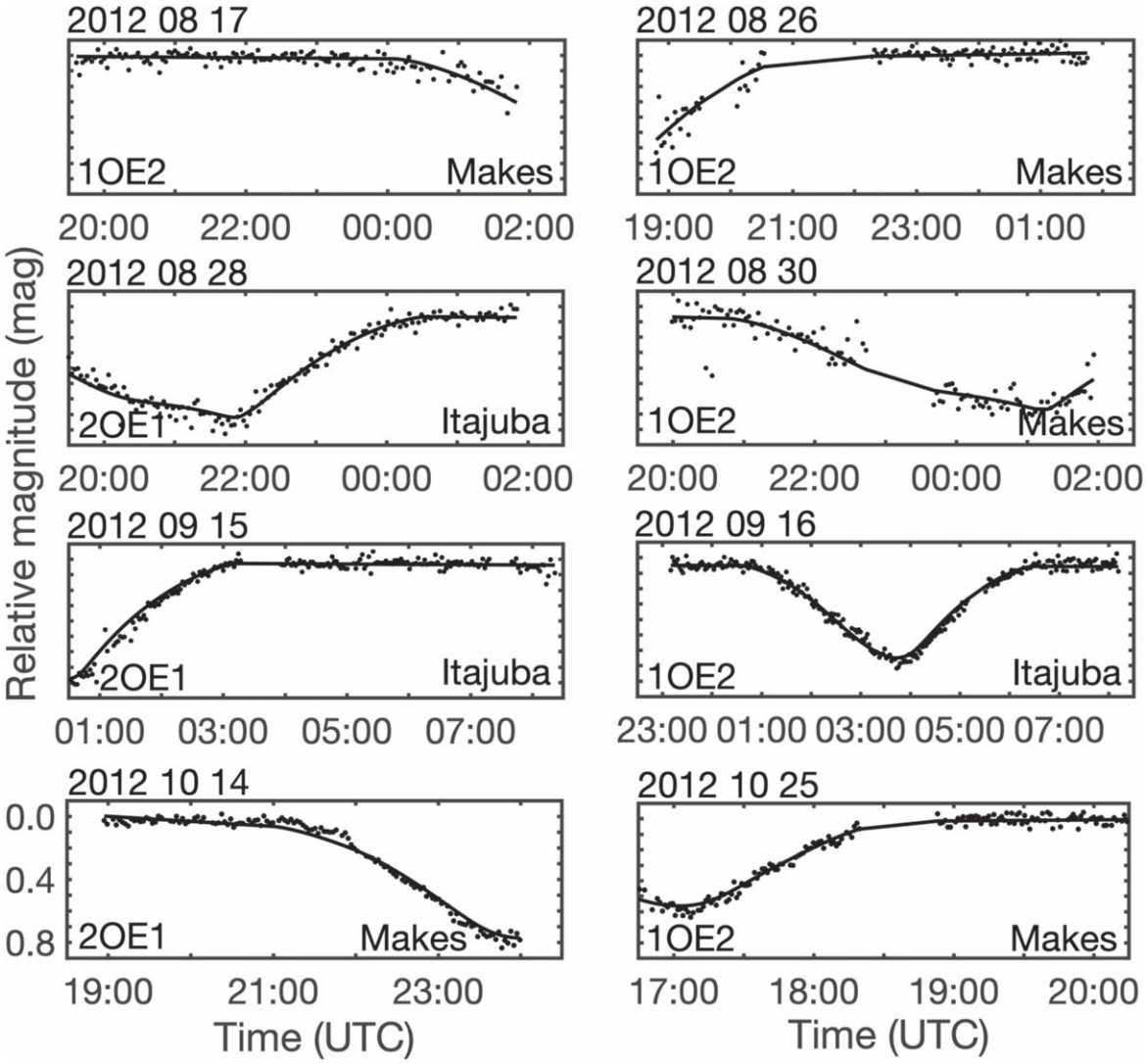

Figure 2. Solid lines represent model fits to the selected mutual events lightcurves from 2012. The vertical dimension is the same for all panels, 0.1 mag. The rest of the lightcurves fits from 2012 are in the Appendix.

easy to flip the system by 180 deg. However, our orbit fit already had a solid estimate of mean motion. A flip in the system would require an error of 180 deg/720 days or $\sim$0.25 deg day^{-1}. An error of this magnitude would have easily been spotted in the 2004–2005 relative astrometry. We continued to add the rest of the data in the sequential order in time.

3. Results

3.1. State Vectors and Residuals

The fitting procedure yielded positions and velocities as shown in Table 1. The system mass was estimated to be $GM = 0.0950 \pm 0.0012$ km^3 s^{-2} or $M_{\rm sys} = 1.424 \pm 0.018 \times 10^{18}$ kg. For comparison, the orbital solution by Grundy et al. (2018) yielded $GM = 0.0941 \pm 0.0019$ km^3 s^{-2} or $M_{\rm sys} = 1.410 \pm 0.029 \times 10^{18}$ kg. It is interesting to note that the mass reported here is still within the bounds of the original paper by Marchis et al. (2006), $M_{\rm sys} = 1.36 \pm 0.11 \times 10^{18}$ kg.

Bulk density will depend on what we assume to be the total volume of the system. Mueller et al. (2010) reported the volume equivalent spherical diameters of $D_P = 106 \pm 11$ km and $D_M = 98 \pm 10$ based on thermal observations, Buie et al. (2015) reported $D_P = 113$ km and $D_M = 104$ km based on stellar occultation (no uncertainties were given), and Berthier et al. (2020) derived their own dimensions of the components (130.8 × 126.2 × 122.8) km and (117.1 × 110.8 × 107.8) km based on inversion of the lightcurves and subsequent size calibration. The resulting volumes are: 1.60×10^6 km^3 for Mueller et al. (2010), 1.36×10^6 km^3 for Buie et al. (2015), and 1.79×10^6 km^3 for Berthier et al. (2020). The last volume is about 24% larger than the volume reported by the stellar occultation analysis. Pinilla-Alonso et al. (2022) recently reported on the potential void on the pole of Menoetius that appears to support Buie et al. (2015) smaller volume. We decided to adopt Buie et al. (2015) volume and to assign a subjective uncertainty of 20% in order to cover for larger models. From here, we obtain a system density of 1.05 ± 0.21 g cm^{-3}. This density uncertainty is dominated by the volume uncertainty, but the overall value is in agreement with all previously published values, within their uncertainties.

The residuals are listed in Table 2. In general, most of the residuals for the 2004–2017 data remained within several mas, and all larger residuals (a few tens of mas) occurred for the data

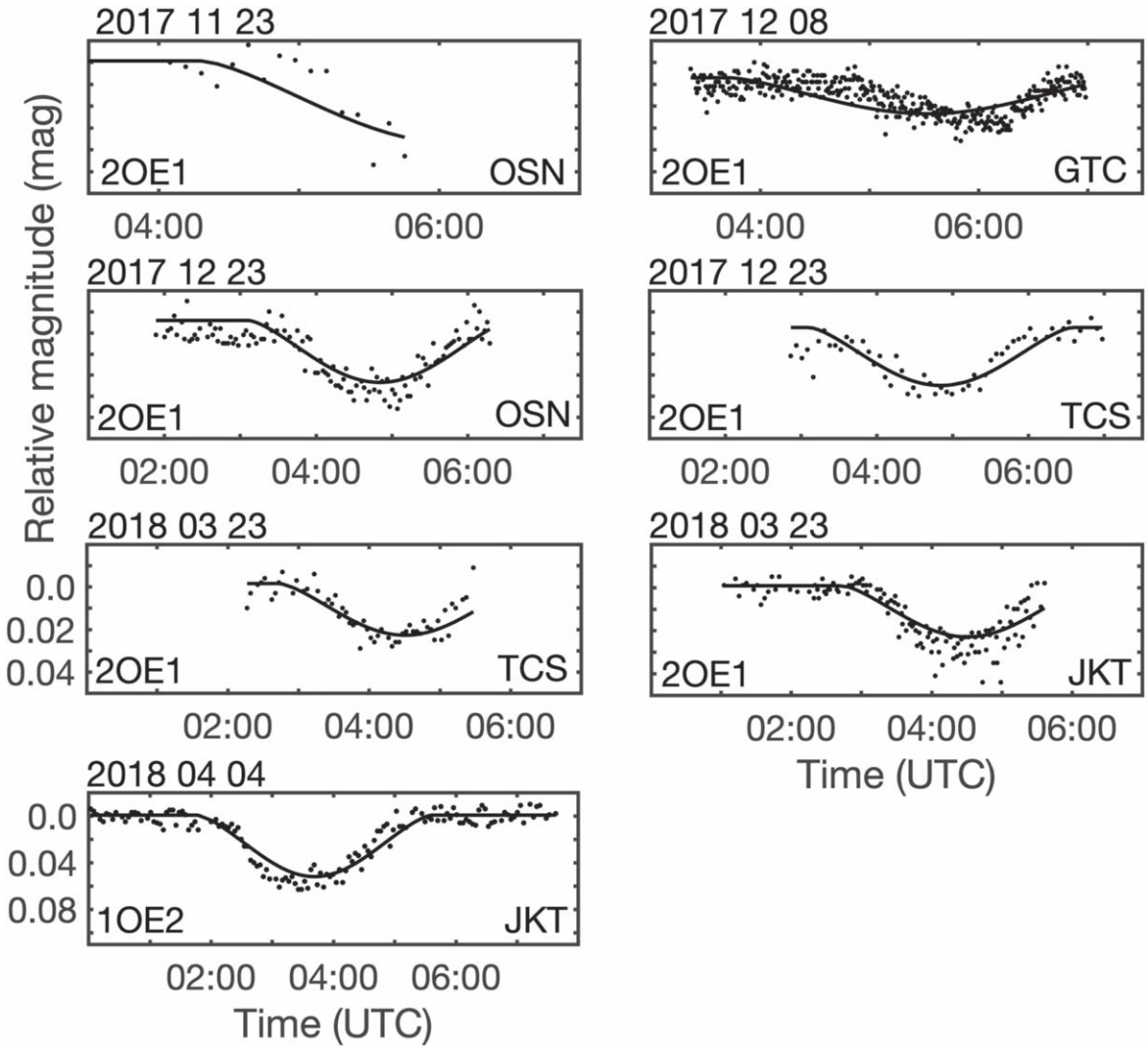

Figure 3. Solid lines represent model fits to all reported mutual events lightcurves from 2017 to 2018 (Pinilla-Alonso et al. 2022). OSN stands for Sierra Nevada Observatory, GTC is Gran Telescopio Canarias, TCS is Telescopio Carlos Sánchez, and JKT is Jacobus Kapteyn Telescope. The vertical dimension is 0.07 mag for all panels except the last one which is 0.11 mag.

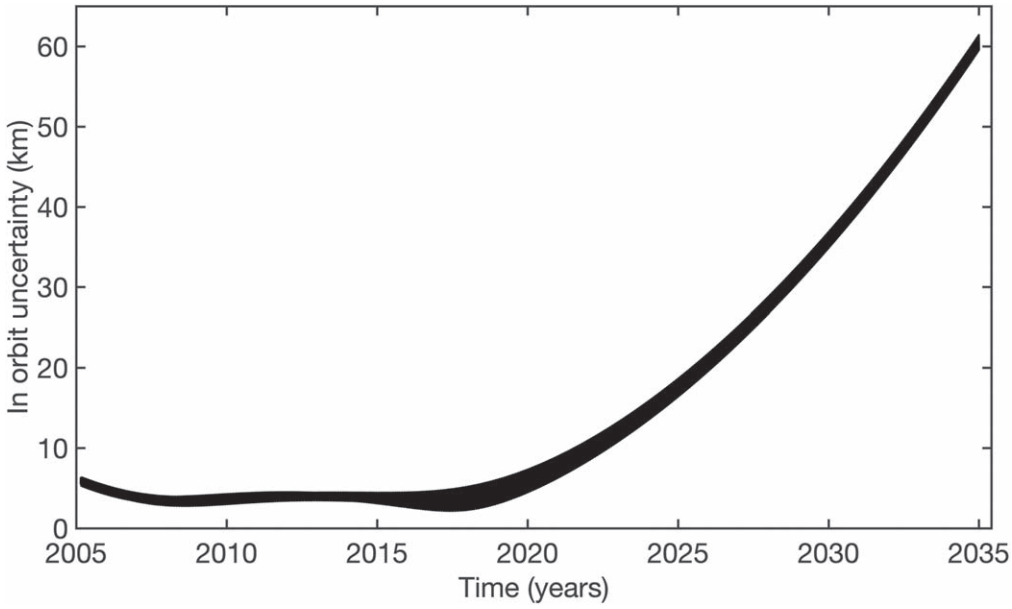

Figure 4. Growth of the in-orbit (along the track) uncertainty over time.

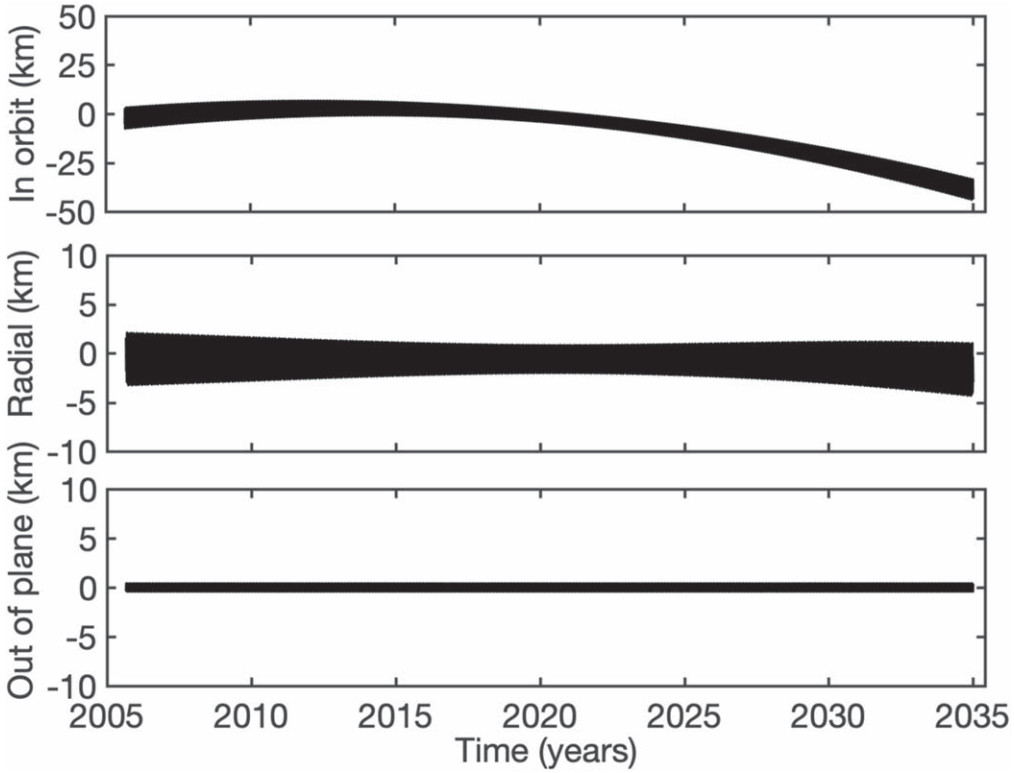

Figure 5. Orbital differences between Keplerian and non-Keplerian solutions.

Table 3
Mutual Events Season 2024—Superior Events

Date (UTC)	Start hh:mm:ss	Stop hh:mm:ss	Event Max hh:mm:ss	Events
2024 09 23-24	19:17	00:51	21:51	PO, PO+PE, PE
2024 09 28	02:15	07:30	04:50	PO, PO+PE, TO, PO+PE, PE
2024 10 02	09:14	14:22	11:50	PO, PO+PE, TO, PO+PE, PO
2024 10 06	16:12	21:20	18:48	PO, PO+PE, TO, PO+PE, PO
2024 10 10-11	23:08	04:18	01:45	PE, PO+PE, TO, PO+PE, PO
2024 10 15	05:52	11:16	08:42	PE, PO+PE, PO
2024 10 19	12:37	18:14	15:40	PE, PO+PE, PO
2024 10 23-24	19:22	01:11	22:37	PE, PO+PE, PO

Note. The first two columns list the start and stop times of mutual events. The third column displays the time when the maximum drop in brightness occurs. The last column represents the sequential events that occur between the start and stop times. Possible events include: PO—Partial Occultation, PE—Partial Eclipse, PO+PE—Partial Occultation and Partial Eclipse with overlap, PO_PE—Partial Occultation and Partial Eclipse without overlap, TO—Total Occultation, and TE—Total Eclipse. The mutual events were modeled using 56.5 and 52 km radii for Patroclus and Menoetius.

(This table is available in its entirety in machine-readable form.)

obtained from 2001 to 2002. This is consistent with the residual statistics reported by Grundy et al. (2018) and Berthier et al. (2020). The two largest weighted residuals occur for the 2017 May 29 and 2017 June 13 data points, but their absolute values are still only ∼5 mas. The root–mean–square (rms) of the weighted residuals are 0.69 and 0.54. This means that the observers weighted their data conservatively. We decided to leave the data weights as they were reported because the astrometry was still sparse and we did not want to risk that weight manipulation introduces some artifacts into the fit. Furthermore, we liked the idea of a slightly inflated covariance, because this produced more conservative uncertainties.

Fits to the lightcurves are shown in Figures 1–3, with the complete set presented in the Appendix. For the 24 superior events, we get the relative albedo of Menoetius to Patroclus of 1.006 ± 0.011 (see Equation (1)). For the 18 inferior events we get the relative albedo of Patroclus to Menoetius of 1.004 ± 0.016. From here, it appears that both objects have very similar albedos. Overall, there is a good correspondence between the model and the data, especially considering that we used spheres in our model and assumed a simple Lambertian scattering. The largest discrepancy occurs for the lightcuve obtained on 2017 December 8. On this date, Menoetius was being occulted by Patroclus in a grazing event. Our orbit fit suggests that the event should have started around 04:00 UTC and the lightcurve clearly shows a start time about an hour later. This particular lightcurve was identified in Pinilla-Alonso et al. (2022) as evidence for the presence of a void on the south

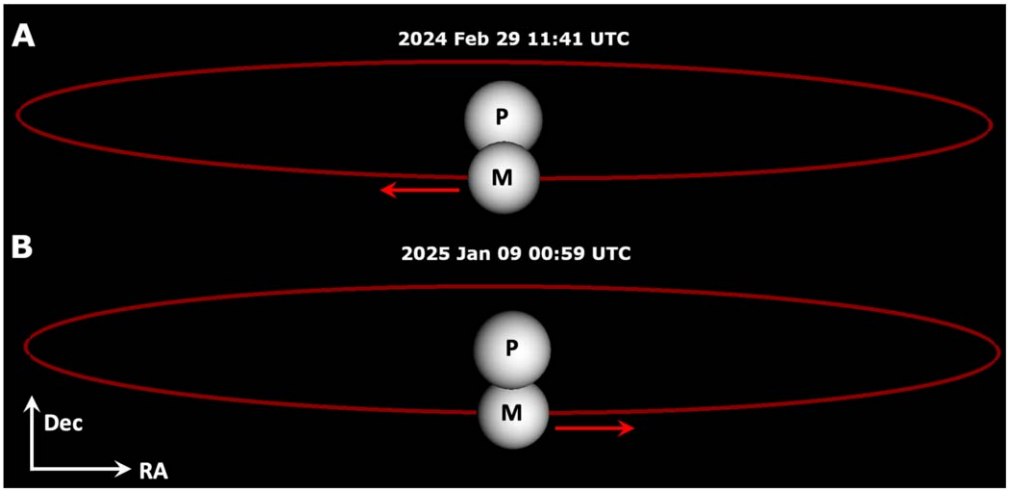

Figure 6. A. The inferior event geometry on the plane of sky on 2024 February 29. B. The superior event geometry on the plane of sky on 2025 Jan 09. Both events are partial occultations. The red arrows indicate the motion of Menoetius with respect to Patroclus. We used the SPICE-enhanced Cosmographia software for the visualizations (Acton et al. 2018).

Table 4
Mutual Events Season 2024—Inferior Events

Date (UTC)	Start hh:mm:ss	Stop hh:mm:ss	Event Max hh:mm:ss	Events
2024 09 21	16:04	21:48	18:45	PO, PO+PE, PE
2024 09 25-26	23:02	04:26	01:41	PO, PO+PE, PE
2024 09 30	06:00	11:09	08:38	PO, PO+PE, AO+PE, PO+PE, PO
2024 10 04	12:58	18:07	15:30	PO, PO+PE, AO+PE, PO+PE, PO
2024 10 08-09	19:57	01:05	22:26	PO, PO+PE, AO+PE, PO+PE, PO
2024 10 13	02:45	08:03	05:24	PE, PO+PE, PO
2024 10 17	09:29	15:01	12:22	PE, PO+PE, PO
2024 10 21	16:14	21:58	19:20	PE, PO+PE, PO

Note. The same caption as for Table 3, except that AO and AE now mark Annular Occultation and Annular Eclipse—events for which the disk/shadow of Menoetius is completely contained within the disk of Patroclus.

(This table is available in its entirety in machine-readable form.)

pole of Menoetius. Although Buie et al. (2015) were the first to report the absence of occultation chords in that region, the hypothesis of a void was dismissed at that time due to possible equipment issues and the lack of such a feature in the available rotational lightcurves.

3.2. Mean Osculating Elements

We used state vectors from the integrated orbits to derive ecliptic osculating elements for 100,000 points from 2005 to 2035. We obtained the following mean elements: $a = 692.5$ km, $e = 0.004$, and $i = 152.4$ deg (with respect to the ecliptic). The ICRF orbital pole corresponds to R.A. $= 178.0$ deg and $\delta = -74.1$ deg. These elements are consistent with the previous works of Marchis et al. (2006) and Grundy et al. (2018).

We estimated orbital uncertainties by mapping the covariance matrix from Cartesian to classical elements space (Jacobson et al. 2012). At the model epoch, 2005 February 26 00:00:00 TDB, we obtained $a = 692.5 \pm 4.0$ km, $e = 0.004 \pm 0.004$, $i = 152.4 \pm 0.2$ deg, R. A. $= 178.0 \pm 0.5$ deg and $\delta = -74.1 \pm 0.2$ deg (1σ errors). For comparison, Grundy et al. (2018) estimated R. A. $= 179.3 \pm 1.8$ deg and $\delta = -74.1 \pm 0.6$ deg. Our uncertainties on the pole direction are smaller because we utilized all available data, whereas Grundy et al. (2018) only used 2013–2017 relative astrometry.

We obtain the average osculating siderial period of $P = 4.282754 \pm 0.000023$ days. The period uncertainty is estimated by measuring the uncertainty in mean motion. We used covariance mapping to assess how the in-orbit uncertainty evolves until 2035 (Figure 4). The mean-motion uncertainty, Δn, can be calculated as $\Delta n = \frac{1}{a}\frac{\Delta y}{\Delta t}$, where $a = 692.5$ km, $\Delta y = 60$ km (in-orbit uncertainty in 2035), and $\Delta t = 30$ yr. This results in an uncertainty of 0.00005 deg day^{-1} in mean motion, and $\Delta P = P/n\Delta n = 2.3 \times 10^{-5}$ days period uncertainty. It is important to note that all previous period values and their uncertainties were based on Keplerian orbit fits while we derived these values from an integrated orbit that contained non-Keplerian terms.

3.3. Orbital Uncertainties at the Time of the LUCY flyby

We also checked orbital uncertainties for Menoetius relative to Patroclus at the time of the LUCY flyby in March 2033. The 3σ uncertainties were 156 km, 15 km, and 16 km, for in-orbit (along track), radial, and out-of-plane directions. For comparison, the latest 3σ geocentric range uncertainty of the

Patroclus–Menoetius barycenter is about 87 km (see JPL solution number 82).

Figure 5 shows in-orbit, radial, and out-of-plane differences between the Keplerian orbit solution and our nominal orbit solution that included J_2 and C_{22} for both components. The most significant variation occurs along track due to a difference in mean motion between the two orbit models. A deviation of fifty kilometers in 2035 is comparable to the orbital uncertainty of sixty kilometers (1σ) (see Figure 4). Figures 4 and 5 demonstrate that the current astrometry data set does not have sensitivity to distinguish between Keplerian and non-Keplerian solutions.

4. Discussion

We generated mutual events predicts for two sets of Patroclus and Menoetius radii: (49 km, 45 km) for the smaller model of the system and (56.5, 52 km) for the larger. It is unlikely that the objects are significantly smaller or larger than this. The two test cases produced slightly different timings of the events, and these differences were used as the uncertainties. The mutual events season begins in February of 2024 and lasts until January of 2025. The smaller model predicted a slightly later start, 2024 February 25, and earlier end, 2025 January 13, while the larger model predicted the first event on 2024 February 16 and the last event on 2025 January 17. The early and late events were all grazing occultations with a short (<1 hr) duration.

We provide the expected sequence of events for our nominal model with larger radii in Tables 3 and 4. These tables indicate the anticipated event types (such as partial occultation, partial eclipse, a combination of partial occultation and eclipse, etc.), but they do not specify exact start–stop times of each subevent. Instead, we only list the overall start and stop times, as well as the time of the maximum drop in magnitude. The average difference in start–stop times between the models with different sizes was ∼25 minutes, but the mid-times remained only several minutes apart. Additionally, we checked the timing differences between the nominal (non-Keplerian) and Keplerian orbit models. In this case, the difference was equivalent to a constant offset of ∼16 minutes, which is expected based on in-orbit differences (due to mean motion) shown in Figure 5.

Patroclus remains within 70 deg from the Sun until early June of 2024. Optical observations are likely to begin before the time of the total eclipses, which occur during the last week of July. The system is in opposition in late September, providing Earth-observers with an edge-on view in October. New moons near opposition occur on September 3, October 3, and November 2. According to our models, there will be three to four total occultations for the superior events during the first two weeks of October and about the same number of annular occultations for the inferior events. The actual number of events will depend on the sizes and shapes of the components.

The best opportunities to detect the shape of Menoetius' southern limb through inferior events occur in late February and early March (Figure 6). Unfortunately, Patroclus is too close to the Sun at that time. The best superior events involving the same limb region will take place in early January 2025 when Patroclus is still more than 70° away from the Sun. These observations will be challenging due to pre-dawn skies and the proximity to the first quarter Moon. An example of a partial occultation event on 2025 January 8–9 from 23:30:00 to 02:29:00 UTC is shown in Figure 6.

5. Conclusions

We present the development of the orbital ephemeris for Menoetius, the satellite of Patroclus, based on all available relative astrometry and mutual events lightcurves. The orbital solution indicates a negligible eccentricity, that has been well constrained through the timing of superior and inferior events. The system mass, $GM = 0.0950 \pm 0.0012$ km^3 s^{-2}, and the siderial orbital period of $P = 4.282753 \pm 0.000023$ days are consistent with the previously published values. We estimated a bulk density of 1.05 ± 0.21 g cm^{-3}(1σ).

We used the latest ephemeris to predict the mutual events season of 2024–2025. The best observing opportunities occur in the second half of 2024, after the system emerges from the bright glare of the Sun. Our analysis demonstrates that we can estimate the start and stop times of the mutual events with an accuracy of approximately 25 minutes. Future observations of the mutual events will further refine the orbit and help investigate topography at the south pole of Menoetius. The non-Keplerian effects are not apparent, but long baseline of observations could eventually lead to their detection.

At the time of the LUCY mission flyby, we estimate that the orbital uncertainties are ∼60 km, primarily along the orbital path. The orbital solution presented here can be obtained from JPL's On-Line Solar System Data Service (Giorgini et al. 1996) and from NASA's Navigation and Ancillary Information Facility website (Acton 1996) as tnosat_v001_20000617_jpl082_20230601.bsp.

Acknowledgments

The research described here was carried out at the Jet Propulsion Laboratory, California Institute of Technology, under contract with the National Aeronautics and Space Administration (80NM0018D004). The authors would like to thank astronomers who contributed with their measurements to this orbital analysis as well as to an anonymous reviewer for their constructive comments.

Appendix
Additional Lightcurves

Figures 7–9 show the rest of the lightcurves used in our orbital fit. Several of these lightcurves capture complete or nearly complete mutual events. We note that our three-circle overlap model successfully reproduces even some complex features observed in the lightcurves from 2007 January 26 to 29. On January 26, Menoetius was occulting and eclipsing Patroclus, while on January 29, the geometry was reversed.

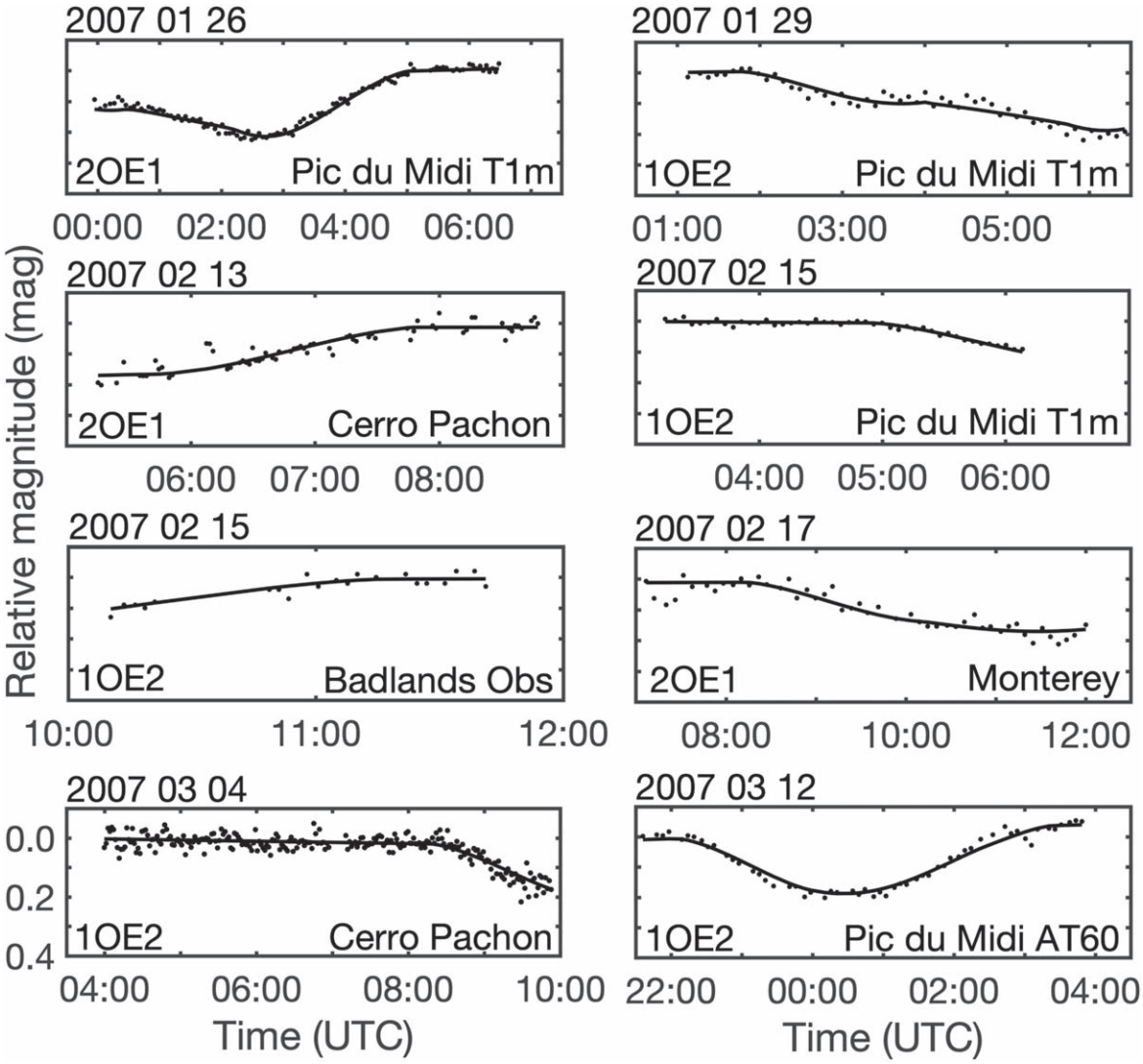

Figure 7. Model fits to the mutual events lightcurves from 2007 January to March.

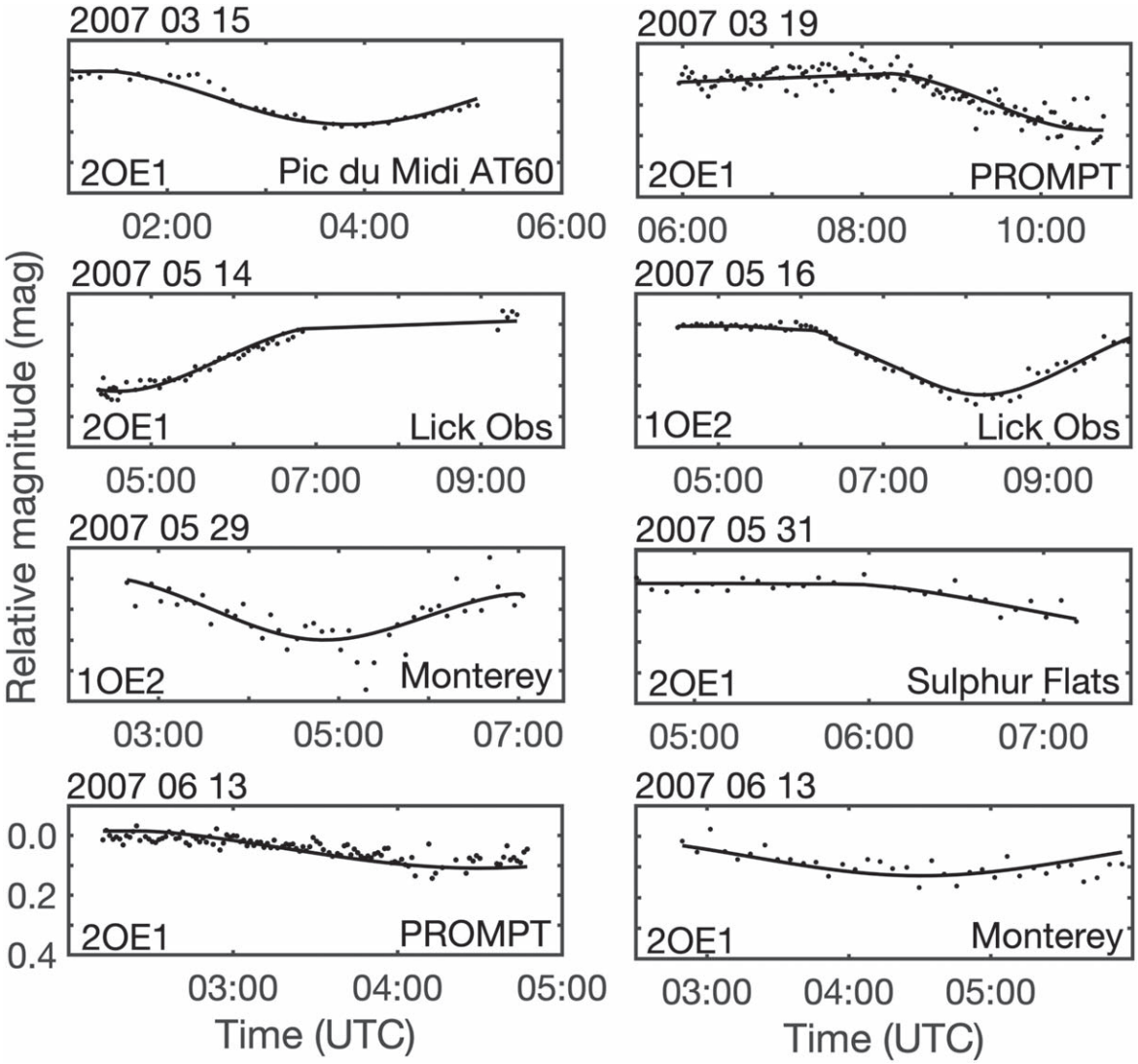

Figure 8. Model fits to the mutual events lightcurves from 2007 March to June.

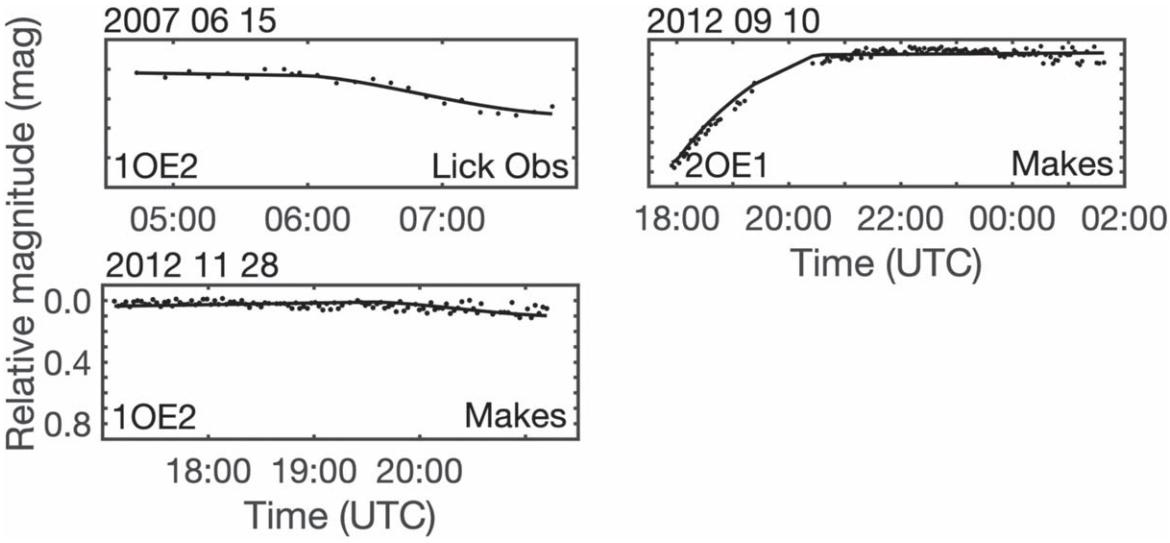

Figure 9. Model fits to the mutual events lightcurves from 2012 June to November.

ORCID iDs

Robert A. Jacobson https://orcid.org/0000-0002-8844-724X
Ryan S. Park https://orcid.org/0000-0001-9896-4585
Jérôme Berthier https://orcid.org/0000-0003-1846-6485
Noemí Pinilla-Alonso https://orcid.org/0000-0002-2770-7896
Marcel Popescu https://orcid.org/0000-0001-8585-204X
Javier Licandro https://orcid.org/0000-0002-9214-337X

References

Acton, C. H. 1996, P&SS, 44, 65
Acton, C., Bachman, N., Semenov, B., & Wright, E. 2018, P&SS, 150, 9
Arlot, J. E., Emelyanov, N. V., Aslan, Z., et al. 2013, A&A, 557, A4
Berthier, J., Descamps, P., Vachier, F., et al. 2020, Icar, 352, 113990
Bierman, G. J. 1977, Factorization Methods for Discrete Sequential Estimation (New York: Academic Press)
Brozović, M., Showalter, M. R., Jacobson, R. A., & Buie, M. W. 2015, Icar, 246, 317
Buie, M. W., Olkin, C. B., Merline, W. J., et al. 2015, AJ, 149, 113
Dunbar, R. S., & Tedesco, E. F. 1986, AJ, 92, 1201
Giorgini, J. D., Yeomans, D. K., Chamberlin, A. B., et al. 1996, BAAS, 28, 1158
Grundy, W. M., Noll, K. S., Buie, M. W., & Levison, H. F. 2018, Icar, 305, 198
Jackson, J. 1924, MNRAS, 84, 602
Jacobson, R., Brozović, M., Gladman, B., et al. 2012, AJ, 144, 132
Lawson, C. L., & Hanson, R. J. 1974, Solving Least Squares Problems (Englewood Cliffs, NJ: Prentice-Hall)
Marchis, F., Hestroffer, D., Descamps, P., et al. 2006, Natur, 439, 565
Merline, W. J., Close, L. M., Siegler, N., et al. 2001, IAU Circ., 7741, 2
Merline, W. J., Weidenschilling, S. J., Durda, D. D., et al. 2002, Asteroids III (Tucson, AZ: Univ. Arizona Press), 289
Morbidelli, A., Levison, H. F., Tsiganis, K., & Gomes, R. 2005, Natur, 435, 462
Mueller, M., Marchis, F., Emery, J. P., et al. 2010, Icar, 205, 505
Murray, C. D., & Dermott, S. F. 1998, Solar System Dynamics (Cambridge: Cambridge Univ. Press)
Nesvorný, D., Youdin, A. N., & Richardson, D. C. 2010, AJ, 140, 785
Noll, K. S., Grundy, W. M., Chiang, E. I., Margot, J. L., & Kern, S. D. 2008, in The Solar System Beyond Neptune, ed. M. A. Barucci et al. (Tucson, AZ: Univ. Arizona Press), 345
Park, R. S., Folkner, W. M., Williams, J. G., & Boggs, D. H. 2021, AJ, 161, 105
Peters, C. F. 1981, A&A, 104, 37
Pinilla-Alonso, N., Popescu, M., Licandro, J., et al. 2022, PSJ, 3, 267
Tapley, B. D., Schutz, B. E., & Born, G. H. 2004, Statistical Orbit Determination (Burlington, MA: Elsevier Academic Press)